7-23-2020

Estimating the Inner Ring Defect Size and Residual Service Life of Freight Railcar Bearings Using Vibration Signatures

Jennifer Lima
The University of Texas Rio Grande Valley

Constantine Tarawneh
The University of Texas Rio Grande Valley, constantine.tarawneh@utrgv.edu

Jesse Aguilera
The University of Texas Rio Grande Valley

Jonas Cuanang
The University of Texas Rio Grande Valley

Recommended Citation

Lima, J, Tarawneh, C, Aguilera, J, & Cuanang, J. "Estimating the Inner Ring Defect Size and Residual Service Life of Freight Railcar Bearings Using Vibration Signatures." Proceedings of the 2020 Joint Rail Conference. 2020 Joint Rail Conference. St. Louis, Missouri, USA. April 20–22, 2020. V001T09A003. ASME. https://doi.org/10.1115/JRC2020-8059

Proceedings of the 2020 Joint Rail Conference
JRC2020
April 20-22, 2020, St. Louis, MO, USA

JRC2020-8059

ESTIMATING THE INNER RING DEFECT SIZE AND RESIDUAL SERVICE LIFE OF FREIGHT RAILCAR BEARINGS USING VIBRATION SIGNATURES

Jennifer Lima
Mechanical Engineering Depart.
The University of Texas Rio Grande Valley
Edinburg, TX, 78539, USA
jennifer.lima01@utrgv.edu

Constantine Tarawneh, Ph.D.
Mechanical Engineering Department
The University of Texas Rio Grande Valley
Edinburg, TX, 78539, USA
constantine.tarawneh@utrgv.edu

Jesse Aguilera
Mechanical Engineering Department
The University of Texas Rio Grande Valley
Edinburg, TX, 78539, USA
jesse.aguilera01@utrgv.edu

Jonas Cuanang
Mechanical Engineering Department
The University of Texas Rio Grande Valley
Edinburg, TX, 78539, USA
jonas.cuanang01@utrgv.edu

ABSTRACT

There are currently two primary wayside detection systems for monitoring the health of freight railcar bearings in the railroad industry: The Trackside Acoustic Detection System (TADS™) and the wayside Hot-Box Detector (HBD). TADS™ uses wayside microphones to detect and alert the train operator of high-risk defects. However, many defective bearings may never be detected by TADS™ since a high-risk defect is a spall which spans about 90% of a bearing's raceway, and there are less than 30 systems in operation throughout the United States and Canada. HBDs sit on the side of the rail-tracks and use non-contact infrared sensors to acquire temperatures of bearings as they roll over the detector. These wayside bearing detection systems are reactive in nature and often require emergency stops in order to replace the wheelset containing the identified defective bearing. Train stoppages are inefficient and can be very costly. Unnecessary train stoppages can be avoided if a proper maintenance schedule can be developed at the onset of a defect initiating within the bearing. Using a proactive approach, railcars with defective bearings could be allowed to remain in service operation safely until reaching scheduled maintenance.

The University Transportation Center for Railway Safety (UTCRS) research group at the University of Texas Rio Grande Valley (UTRGV) has been working on developing a proactive bearing condition monitoring system which can reliably detect the onset of bearing failure. Unlike wayside detection systems, the onboard condition monitoring system can continuously assess the railcar bearing health and can provide accurate temperature and vibration profiles to alert of defect initiation. This system has been validated through rigorous laboratory testing at UTRGV and field testing at the Transportation Technology Center, Inc. (TTCI) in Pueblo, CO. The work presented here builds on previously published work that demonstrates the use of the onboard condition monitoring system to identify defective bearings as well as the correlations developed for spall growth rates of defective bearing outer rings (cups). The system first uses the root-mean-square (RMS) value of the bearing's acceleration to assess its health. Then, an analysis of the frequency domain of the acquired vibration signature determines if the bearing has a defective inner ring (cone) and the RMS value is used to estimate the defect size. This estimated size is then used to predict the residual life of the bearing. The methodology proposed in this paper can assist railroads and railcar owners in the development of a proactive and cost-efficient maintenance cycle for their rolling stock.

INTRODUCTION

Freight railcars (wagons) are supported by a basic set of suspension components which include springs, dampers, axles, wheels, and tapered-roller bearings. Due to the heavy loads that they support while traveling at speeds of up to 113 km/h (70 mph), railroad bearings are susceptible to failure which, if not detected early, may lead to journal burn-off and consequent derailment. Tapered-roller bearings typically consist of rollers, inner rings (cones), outer ring (cup), spacer ring, wear rings, and seals, as illustrated in Figure 1 [1]. Under normal operating

conditions, these tapered-roller bearings provide near-frictionless operation. However, when any of the rolling surfaces within the bearing develops a defect, the near-frictionless quality is compromised, and depending on the size, location, and nature of the defect, this can result in rapid wear from the added frictional heating, and may lead to catastrophic failure of the bearing if not detected early.

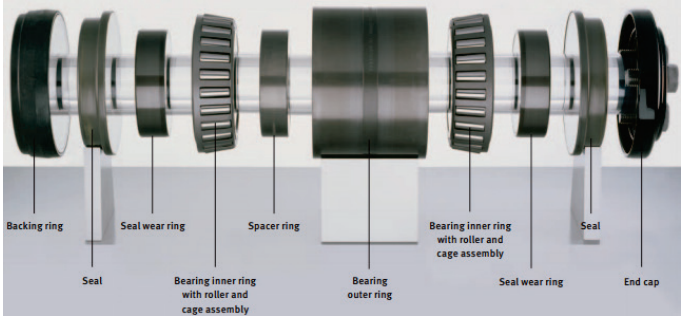

Figure 1. Tapered roller bearing components [1].

Defects in bearings are generally classified under three categories; i.e., local, distributed, and geometric. Localized defects are small pits, cracks, or spalls that develop on one rolling surface, as pictured in Figure 2 (left). A distributed defect is one that spans major portions of one or more rolling surfaces. Localized defects present on multiple rolling surfaces of one bearing are considered to be a distributed defect. The water-etch cone (inner ring) shown in Figure 2 (right) is a prime example of a distributed defect. Out of tolerance bearing components and other geometric and manufacturing irregularities present on the rolling surfaces of the bearing are examples of geometric defects.

Figure 2. Examples of localized defects (left) and distributed defect (right).

In freight rail service, there are two commonly used wayside detection systems for monitoring the condition of freight railcar bearings; namely, the Hot-Box Detector (HBD) and the Trackside Acoustic Detection System (TADS). TADS™ uses a series of wayside microphones to listen to bearings noise signatures as they pass by the detector. While the system is proficient in detecting bearings that are near the end of their service life (i.e., bearings with spalls spanning across 90% of the rolling surfaces which are termed 'growlers'), TADS™ cannot detect small defects in the bearings [2]. Moreover, there are only about 30 of these units in use in North America, most of which are located in the East [3]. Thus, one can presume that many bearings in service may spend their entire service life without going through one of the TADS™ stations, and those that do will go undetected if they contain defects that are relatively small.

HBDs are the most utilized wayside detection systems in the U.S. and Canada, with more than 6000 units in operation in North America [4]. HBDs are typically placed every 25 to 40 rail miles (40 – 64 km), and as the railcar passes over the system, a series of non-contact infrared sensors measure the temperatures emitted from the bearings, wheels, axles, and the brakes. If the operating temperature of any bearing is 94.4°C (170°F) above ambient or if the temperature difference between two bearings that share the same axle is greater than 52.8°C (95°F), the HBD system will alert the train operator so that proper action can be taken [5]. Over the past two decades, several railroads have adopted a new methodology for using the HBDs in which the individual bearing operating temperatures are systematically compared to the average operating temperature of all the bearings on the same side of the train [5]. If the bearing operating temperature is significantly higher than the average operating temperature of all bearings on the same side of the train as measured by a few consecutive HBDs, the bearing is said to be 'warm trending' and is flagged without setting off any of the HBD alarms explained earlier. 'Warm trending' bearings are removed from rail service for later disassembly and visual inspection. However, a study carried out by Amsted Rail concluded that nearly 40% of bearings flagged by HBDs, in the period from 2001 to 2007, were found to have no discernable defects upon inspection. These 'non-verified' bearings are responsible for many costly delays resulting from unnecessary train stoppages. Furthermore, statistics reveal that wayside HBDs failed to detect 151 defective bearings in North America in the period from 2009 to 2018, all of which resulted in catastrophic derailments [6].

In 2016, the UTCRS research team conducted an investigation that compared the temperature profiles of healthy (defect-free) bearings to those with a defective inner (cone) and outer (cup) rings [7]. The study concluded that the operating temperature was not a good indicator of bearing health because bearings with defective inner and outer rings had operating temperatures that were comparable to those of healthy bearings. Hence, the UTCRS research team focused on the development of an advanced onboard condition monitoring system that utilizes both accelerometers and temperature sensors to assess bearing health [8]. This system has been validated through extensive laboratory testing and an on-track field test carried out at TTCI and has proven to be a reliable and accurate bearing condition monitoring system capable of detecting the onset of defect initiation within the bearing. Coupled with prognostics models developed for spall growth rates on bearing cups and cones [9], the onboard condition monitoring system can estimate the approximate defect size and the residual bearing service life. Previous work performed by the authors demonstrated how the condition monitoring algorithm was used to estimate the residual service life for bearings with outer ring (cup) defects [10]. The current study will present a methodology for estimating inner ring (cone) defect size and the residual bearing service life.

EXPERIMENTAL SETUP & PROCEDURES

Two different bearing dynamic test rigs were used to perform the experiments for this study; namely, the four-bearing tester (4BT) pictured in Figure 3 (right), and the single bearing tester (SBT) pictured in Figure 3 (left). The four-bearing tester is housed in an environmental chamber that can mimic ambient conditions as low as -40°C (-40°F) and as high as 65.6°C (150°F). Both testers are powered by a 22 kW (30 hp) variable speed motor that is controlled via a variable frequency drive (VFD) that can simulate train traveling speeds in the range of 8 to 137 km/h (5 to 85 mph). The vertical load, in both testers, is applied by a 18 cm (7 in) diameter hydraulic cylinder that is capable of applying loads of up to 150% of the full load (full load being 153 kN or 34.4 kips per bearing for a class F or K bearing). As the name implies, the four bearing tester can accommodate four class K (6½"×9") or class F (6½"×12") tapered roller bearings pressed onto a 4140 steel axle, whereas, the single bearing tester can only accommodate one class F or K bearing that is cantilevered at the end of a specially fabricated 4140 steel axle. However, unlike the four-bearing tester, the single bearing tester can also apply lateral and impact loads to mimic forces acting on the bearing as a result of the railcar negotiating curves on the track and forces resulting from wheel impacts or bad track segments. Finally, both testers employ two large industrial size fans to provide convective cooling over the test bearings simulating the air cooling that takes place when a train is in motion. The fans generate an average airflow of about 6 m/s (13.4 mph). A schematic of the top view of the four-bearing tester is presented in Figure 4.

Figure 3. Single bearing test rig (left) and four-bearing test rig (right).

The experiments performed for this study were mostly run at full speed of 137 km/h (85 mph) and loads simulating a full railcar (100% load) and an overloaded railcar (125% load). Since the single bearing test rig allows for easier assembly and disassembly of the test bearing, it was used to perform experiments on bearings with spalls having areas greater than 6.45 cm^2 (1 in^2) that required frequent teardowns and inspections to closely monitor the defect progression. In experiments conducted utilizing the four-bearing test rig, only data acquired from the two middle bearings were used in the analysis of the results. This is due to bearing 2 (B2) and bearing 3 (B3) being top loaded, which is the case in rail service. The two end bearings, bearing 1 (B1) and bearing 4 (B4), are bottom-loaded and, hence, only healthy control bearings are placed in these two locations. Figure 5 is a schematic showing the bearing rotation relative to the loaded and unloaded zones of the bearing.

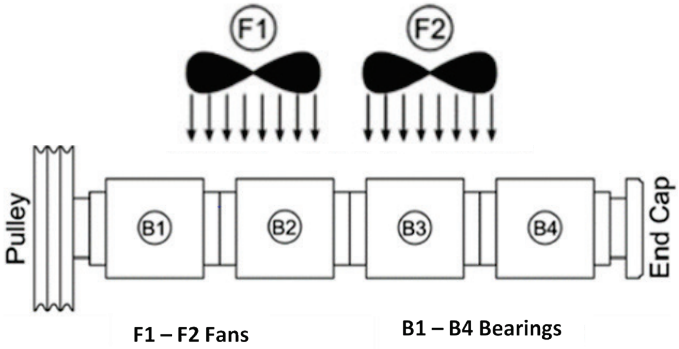

Figure 4. Top view of four-bearing tester (4BT).

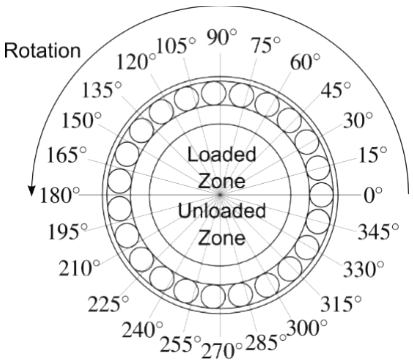

Figure 5. Bearing schematic showing direction of rotation relative to loaded and unloaded zones of the bearing.

During testing, the outer ring (cup) of the bearing remains static while the inner rings (cones) of the bearing rotate in unison with the test axle. Hence, cones containing spalls will cycle between the loaded and unloaded zones of the bearing. In order to minimize crosstalk in the accelerometers resulting from spalls on one bearing affecting the accelerometer signal on the adjacent bearing, the cones containing spalls are placed as far as possible from one another. So, referring to Figure 4, one spalled cone would be placed on the inboard side of bearing 2 (B2) which is closest to bearing 1 (B1) while the other spalled cone would be placed on the outboard side of bearing 3 (B3) which is closest to bearing 4 (B4). This will ensure the least possible crosstalk between the accelerometers. In experiments performed using the single bearing test rig, the spalled cones are usually placed on the inboard raceway of the bearing.

Vibration and temperature data are acquired from the test bearings using accelerometers and thermocouples, respectively.

The steel adapters for the two middle bearings in the four-bearing tester were machined to accept two 70g accelerometers placed in the outboard smart adapter (SA) and mote (M) locations, one 500g accelerometer placed in the outboard radial (R) location, two K-type bayonet thermocouples placed in the middle of each raceway, and one regular K-type thermocouple held tightly in place by a hose clamp. Figure 6 shows the modified bearing adapter as well as the different locations of the three accelerometers and the three thermocouples. In Figure 6, "R" stands for the "Radial" location, "M" stands for the "Mote" location, and "SA" stands for the "Smart Adapter" location.

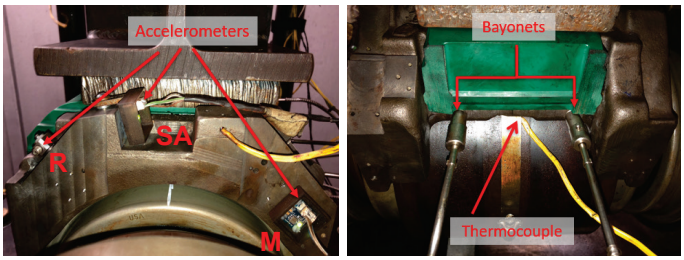

Figure 6. Modified bearing adapter showing vibration sensors (left) and temperature sensors (right).

A similar process was followed for the adapter used in the single bearing tester. The steel adapter was machined to accept four 70g accelerometers placed in the SA and M locations at both the inboard and outboard sides of the bearing, and one 500g accelerometer placed in the R location on the outboard side. For temperature monitoring, four bayonet thermocouples (two inboard and two outboard) were affixed to the bearing adapter as well as seven standard K-type thermocouples placed equidistantly around the circumference of the bearing outer ring (cup) held tightly in place via a hose clamp, as shown in the picture of Figure 7.

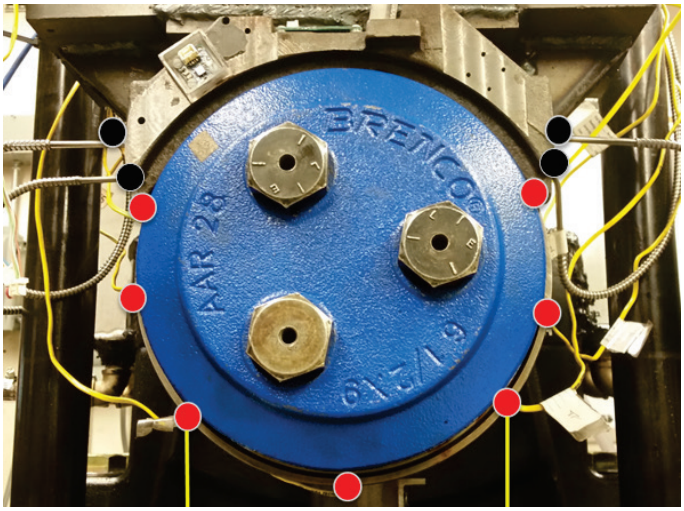

Figure 7. Bearing thermocouple locations: standard K-type thermocouples represented by red dots, bayonet-style thermocouples represented by black dots.

A National Instruments (NI) PXIe-1062Q data acquisition system (DAQ) programmed using LabVIEW™ was used to acquire vibration and temperature data during testing. A NI TB-2627 and 8-channel NI PXI-4472B cards were used to collect and record thermocouple (temperature) and accelerometer (vibration) data, respectively. Temperature data was collected at a sampling rate of 128 Hz for half a second in 20-second intervals. Vibration data was recorded from the accelerometers at a sampling rate of 5,120 Hz for 16 seconds in 10-minute intervals. The root-mean-square (RMS) of the accelerometer data was then used to perform the vibration analyses presented in this paper.

Once the detected vibration levels within a test bearing are above the typical threshold value for healthy bearings, the experiment is stopped, the bearings are then pressed off the axle, disassembled, and cleaned for a thorough visual inspection of the components. If a new spall has formed on any of the raceways or a pervious spall has propagated, a casting is created by first surrounding the defective area with sealant tape capable of withstanding temperatures of up to 204°C (400°F). A molten bismuth alloy, with a melting temperature of 80°C (176°F), is then poured into the mold created by the sealant tape, as pictured in Figure 8. After the bismuth hardens, the casting is removed from the mold and the spalled region reflected on the casting is painted to highlight the defect. Creating a casting of the defect helps track spall propagation once the bearing is reassembled and pressed onto the axle to resume testing. The casting also aids in obtaining a precise measurement of the defect area. This is accomplished by taking an image of the casting with the painted spall which is then post-processed utilizing codes created in MATLAB™ that enhance the contrast of the darkened spall region. The image is then imported to Image Pro-Plus® where a digital analysis of the defect region is performed through optical techniques to acquire accurate defect area parameters.

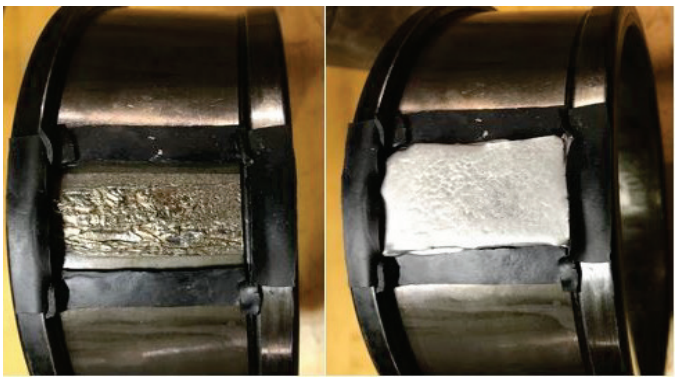

Figure 8. Casting procedure using bismuth and sealant tape

RESULTS AND DISCUSSION

For this study, results acquired from previous work were used to get estimates of the residual service life of bearings with inner ring (cone) defects. The data provided in Table 1 was obtained from a previous study where the spall growth rates for defective inner rings (cones) were calculated by means of a

defect area versus mileage correlation [9]. Table 1 provides the minimum, maximum, and average cone spall growth rates for spall sizes below and above 6.45 cm^2 (1 in^2). The bearing vibration level data (i.e., RMS values) along with the defect area growth rates were used to estimate the defect size and the residual service life of the bearing. Figure 9 provides an experimentally acquired correlation that relates the RMS values of vibration in [g] to the cone spall area in [cm^2] at operating conditions of 137 km/h (85 mph) and loads of 100% and 125% of full load. The data summarized in Table 1 and Figure 9 has been collected from numerous experiments performed over the span of a decade.

Table 1. Spall growth rates of defective inner rings (cones).

Spall Size	Minimum Growth Rate [cm^2/km]	Average Growth Rate [cm^2/km]	Maximum Growth Rate [cm^2/km]
< 6.45 cm^2	0.001×10^{-4}	0.35×10^{-4}	1.74×10^{-4}
> 6.45 cm^2	0.42×10^{-4}	0.68×10^{-4}	1.28×10^{-4}

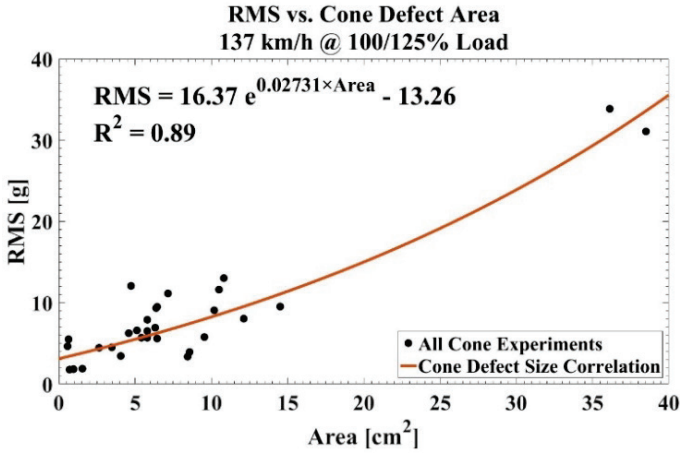

Figure 9. RMS versus cone spall area correlation.

Example Case: Laboratory Experiment 209

In Experiment 209, a bearing having a spall on its inboard cone (inner ring) raceway was placed in the B2 location (refer to Figure 4) of the four bearing tester. The cone raceway spall, pictured in Figure 10 (left), had an initial area of 4.58 cm^2 (0.71 in^2). During the experiment, the test bearings ran a total distance of 122,006 km (75,811 mi), in which the defect area propagated to 5.16 cm^2 (0.80 in^2), as depicted in Figure 10 (right). This new spall area constitutes only 1.85% of the total cone raceway surface area of 279.10 cm^2 (43.26 in^2).

The vibration and temperature profiles of bearing B2 for Experiment 209 are presented in Figure 11. The vibration level data as measured by the RMS values in [g] acquired from the Smart Adapter (SA) and Mote (M) location accelerometers (refer to Figure 6) are plotted. The bearing operating temperatures above ambient conditions are also provided, where the ambient temperature in the laboratory was maintained at 20°C (68°F). Examining the vibration signatures of B2, one can notice that the RMS value started to increase at around 150 hours into the experiment as exhibited by both accelerometers. This increase continued until the RMS value read by the B2-M accelerometer exceeded the maximum threshold value indicated by the solid red line in Figure 11. The increase in the RMS value is a direct result of the defect propagating and introducing metal debris into the bearing, which disrupts the normal operation of the rolling surfaces. With continued operation, the metal debris gets grinded into much smaller pieces due to the forces exerted by the rolling elements and, thus, the RMS values tend to settle or slightly decrease once all debris is crushed, as exhibited by the RMS values after 350 hours into the test. In general, this cycle continues as the defect propagates.

Figure 10. Initial cone raceway spall (left) and final cone spall (right) for bearing B2 in Experiment 209.

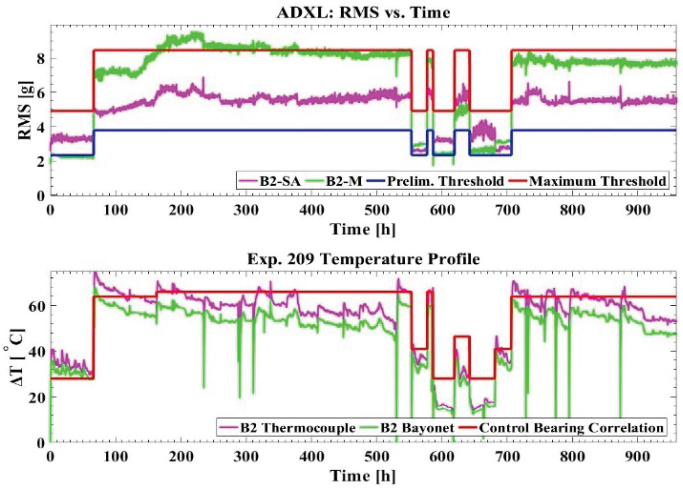

Figure 11. Vibration and temperature profiles for Experiment 209. The bearing operating temperature above ambient is plotted where the ambient temperature is 20°C (68°F).

Interestingly, while the vibration levels within the bearing undoubtedly indicate that the defect has propagated, the temperature profile does not show any signs of abnormal behavior. Except for the initial grease break in period and instances immediately following a sudden change in operating conditions, the operating temperature of the bearing is well within the control (healthy) bearing threshold indicated by the solid red line. One can argue that the bearing operating temperature decreases slightly throughout the duration of the experiment. These results agree with previous observations from

earlier studies [7]. The decrease in bearing operating temperature is believed to be the result of the spall region acting as a cavity in which grease accumulates and provides additional convective cooling to the rolling elements.

The correlation given in Figure 9 was used to estimate the defect size (spall area) based on the average RMS value over the last two hours of testing in Experiment 209. For convenience, the average RMS and bearing operating temperature above ambient values are provided in Table 2. Note that the average RMS value listed in Table 2 was calculated for the Smart Adapter (SA) location accelerometer (B2-SA) since the correlation of Figure 9 was obtained using accelerometers placed in the SA location. The estimated defect size along with the estimation percent error and the calculated growth rate in [cm^2/km] for this experiment are presented in Table 3. The estimated spall area of 5 cm^2 (0.78 in^2) is only 3.1% off from the actual spall area measured during the visual inspection of the spall following Experiment 209. This accuracy is remarkable given that the spall area occupies only 1.85% of the total cone raceway surface area. Moreover, the calculated spall area growth rate seems to be in line with the values provided in Table 1.

Table 2. Average values for the final two hours of Experiment 209 (Average ambient temperature was 20°C or 68°F)

Track Speed [km/h] / [mph]	Load [%]	B2 ΔT [°C / °F]	Control ΔT [°C / °F]	RMS [g]
137 / 85	100	50.2 / 90.4	64.0 / 115.2	5.5

Table 3. Defect size (spall area) estimations and spall growth rate for Bearing 2 in Experiment 209

Average RMS [g]	Actual Defect Size [cm^2]	Estimated Defect Size [cm^2]	Percent Error [%]	Calculated Growth Rate [cm^2/km]
5.5	5.16	5.00	3.1	0.05×10^{-4}

Based on this defect size and the growth rate data presented in Table 1, if the average growth rate value of 0.35×10^{-4} cm^2/km were used, it would take this defect approximately 3,839,714 km (2,385,894 mi) of operation to spread across 50% of the entire cone raceway surface area. Even using the maximum growth rate value of 1.74×10^{-4} cm^2/km, it would still take 772,356 km (479,921 mi) for the spall to propagate to 50% of the entire cone raceway surface area. Thus, this implies that if the defect (spall) is identified at its early stages, the railcar owner/operator will have plenty of time to schedule proactive maintenance and avoid unnecessary and costly train stoppages and delays.

Example Case: Laboratory Experiment 202

Experiment 202 was carried out on the single bearing test rig (SBT) using a class K bearing with a defective inner ring (cone) placed in the inboard location of the test bearing. The test bearing ran a total distance of 40,050 km (24,886 mi) during which the spall area propagated from an initial size of 10.51 cm^2 (1.63 in^2), as pictured in Figure 12 (left), to an area of 10.82 cm^2 (1.68 in^2), as depicted in Figure 12 (right). This represents a calculated spall growth rate of about 0.08×10^{-4} cm^2/km, which is lower than the values listed in Table 1.

Figure 12. Initial cup spall (left) and final cup spall (right) for Experiment 202. [ruler in inches]

The vibration and temperature profiles for Experiment 202 are plotted in Figure 13. As was the case in Experiment 209, the bearing operating temperature remained well below the threshold for control bearings indicated by the solid red line. The latter confirms that the operating temperature is not a good indicator of bearing health. In contrast, the vibration signature of the test bearing of Experiment 202 clearly indicates that the bearing is defective since the RMS values of both accelerometers (IB-SA and IB-M) are mostly above the maximum threshold value for healthy bearings specified by the solid red line in Figure 13. This becomes apparent in the periods between 240 and 280 hours and after 450 hours into Experiment 202. Table 4 summarizes the average bearing operating temperature and IB-SA accelerometer RMS value over the last two hours of Experiment 202.

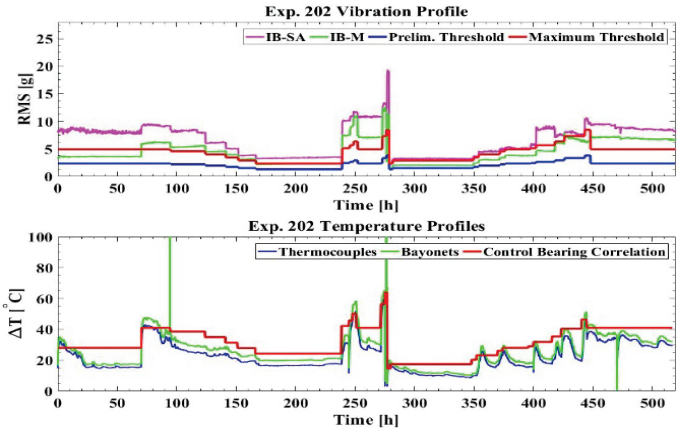

Figure 13. Vibration and temperature profiles for Experiment 202. The bearing operating temperature above ambient is plotted where the ambient temperature is 20°C (68°F).

The RMS value of Table 4 along with the correlation of Figure 9 were used to estimate the defect size of the test bearing. The results are presented in Table 5 along with the estimation percent error and the calculated spall growth rate. Again, the

defect size estimate of 10.1 cm^2 is only 6.6% off from the actual spall area measured during the visual inspection of the bearing, which is noteworthy considering that this defect size represents only 3.9% of the total cone raceway surface area.

Table 4. Average values for the final two hours of Experiment 202 (Average ambient temperature was 20°C or 68°F)

Track Speed [km/h] / [mph]	Load [%]	Bearing ΔT [°C / °F]	Control ΔT [°C / °F]	RMS [g]
137 / 85	100	30.9 / 55.6	41.0 / 73.8	8.3

Table 5. Defect size (spall area) estimations and spall growth rate for test bearing in Experiment 202

Average RMS [g]	Actual Defect Size [cm^2]	Estimated Defect Size [cm^2]	Percent Error [%]	Calculated Growth Rate [cm^2/km]
8.3	10.82	10.1	6.6	0.08×10^{-4}

Finally, as was done for the defect of Experiment 209, if the average growth rate value of 0.68×10^{-4} cm^2/km were used, it would take the defect of Experiment 202 about 1,893,088 km (1,176,313 mi) of operation to spread across 50% of the 279.10 cm^2 (43.26 in^2) total cone (inner ring) raceway surface area. Even using the maximum growth rate value of 1.74×10^{-4} cm^2/km, it would still take 739,828 km (459,709 mi) for the spall (defect) to propagate to 50% of the entire cone raceway surface area, thus, leaving ample time for the railcar owner/operator to schedule proactive maintenance and avoid fines and delays.

CONCLUSIONS

Hot-Box Detectors (HBDs) monitor bearing health through infrared sensors which measure a bearings temperature as the railcar passes over the detector. Temperature-based defect-detection methods are not effective at identifying bearing defects at their early stages of development since bearings with relatively small defects operate at temperatures that are similar to those of healthy bearings. Failure to detect bearing defects can lead to catastrophic derailments. HBDs are reactive in nature since the operating temperature of defective bearings does not rise to the HBD alarm levels until the bearing is near the end of its life and failure is impending.

TADS™ are designed to identify defective bearing in which the defect covers about 90% of the rolling raceway surface area; i.e. “growlers”. These bearings are near the end of their service life, thus, a bearing flagged by TADS™ must be removed from service immediately, which results in costly train stoppages and delays. Moreover, the scarcity of TADS™ units in service limits their benefits in the rail industry.

Bearing health monitoring can be more efficient if proactive maintenance schedules were possible. To this end, the UTCRS research team developed an onboard vibration-based bearing health monitoring system that can accurately and reliably identify the onset of defect initiation within any of the rolling surfaces. Using previously developed correlations for spall area versus RMS values and experimentally acquired spall growth rate data, the onboard condition monitoring algorithm can estimate the defect size within 10% and predict the bearing residual service life so proactive maintenance can be scheduled.

In this paper, two cases were presented for two different test bearings each having a spall on the raceway of one of its cones (inner rings). The results from these two cases demonstrate the usefulness and efficacy of the onboard condition monitoring system in identifying spalls at their very early stages of development and estimating their defect area. The defect area along with the cone spall growth rate data is then used to predict the remaining service life of the bearing. In both cases, the algorithm predicts that the bearing can operate at least 700,000 km (~435,000 mi) before these cone defects in their early stages of development become problematic. This affords the railcar owner/operator enough time to schedule proactive maintenance way before the defective bearing triggers any alarms that result in unnecessary and costly train stoppages and delays.

ACKNOWLEDGMENTS

This study was made possible by funding provided by The University Transportation Center for Railway Safety (UTCRS), through a USDOT Grant No. DTRT 13-G-UTC59.

REFERENCES

[1] "Tapered Roller Bearing Units TAROL Products and Services." Schaeffler. [Online]. [Accessed 12 December 2016]. http://www.schaeffler.com/remotemedien/media/_shared_media/08_media_library/01_publications/schaeffler_2/tpi/downloads_8/tpi_155_de_en.pdf

[2] G.B. Anderson, 2007. “Acoustic detection of distressed freight car roller bearings.” *Proceedings of the 2007 JRCICE Spring Technical Conference*, Pueblo, CO, March 13-16.

[3] G. Fry, 2017. AAR Strategic Research Initiatives Program to Improve Safety and Efficiency. Report prepared by the Transportation Technology Center, Inc.

[4] Predikto: predicting hot box detector failures [Internet]. [cited 2018 Oct 10]. Available from: https://www.predikto.com/download/Predikto_CaseStudy_Railroad_HBD.pdf

[5] S. Karunakaran and T.W. Snyder, 2007. “Bearing temperature performance in freight cars.” *Proceedings Bearing Research Symposium, sponsored by the AAR Research Program in conjunction with the ASME RTD Fall Conference*, Chicago, IL, September 11-12.

[6] Federal railroad administration office of safety analysis. [Internet]. [cited 2019 Feb 21]. Available from: https://safetydata.fra.dot.gov/OfficeofSafety/default.aspx

[7] C. Tarawneh, L. Sotelo, A. Villarreal, N. De Los Santos, R. Lechtenberg, and R. Jones, 2016. “Temperature profiles of railroad tapered roller bearings with defective inner and

outer rings." *Proceedings of the 2016 Joint Rail Conference*, Columbia, SC, April 12-15.

[8] J. Montalvo, C. Tarawneh, and A. Fuentes, 2018. "Vibration-based defect detection for freight railcar tapered-roller bearings." *Proceedings of the 2018 ASME Joint Rail Conference*, Pittsburgh, PA, April 18-20.

[9] C. Tarawneh, J. Lima, N. De Los Santos, and R. Jones, 2019. "Prognostics models for railroad tapered-roller bearings with spall defects on inner or outer rings." *Tribology Transactions*, 62:5, pp. 897—906. https://doi.org/10.1080/10402004.2019.1634228

[10] J. Montalvo, C. Tarawneh, J. Lima, J. Cuanang, and N. De Los Santos, 2019. "Estimating the outer ring defect size and remaining service life of freight railcar bearings using vibration signatures." *Proceedings of the 2019 ASME Joint Rail Conference*, Snowbird, UT, April 9-12.